

Prof. Ian Meiklejohn of the Department of Geography, Geoinformatics and Meteorology of the University of Pretoria, did his PhD degree on rock weathering in Main Caves, Giant's Castle. Since then, in collaboration with Prof. Kevin Hall (Geography Department, University of Northern British Columbia, Canada) he has continued with studies on rock weathering and its impact on San rock art in the Ukhahlamba Drakensberg Park. The rock fragment that I analysed in this study was collected by them in the course of their research and the reference samples I used in the study I collected on one of their field trips to the Giant's Castle area.

Werner Barnard, a PhD student in the Chemistry department, did his MSc thesis on carotenoid pigments and wrote the paragraph on bacterioruberin.

The work were presented by myself as an oral contribution at the *4th International Conference on the Application of Raman Spectroscopy in Art and Archaeology* held in Modena, Italy, 3 – 7 Sept. 2007 and published in the Journal of Raman Spectroscopy.

Linda C Prinsloo, Werner Barnard, Ian Meiklejohn and Kevin Hall, The first Raman spectroscopic study of San rock art in the Ukhahlamba Drakensberg Park, South Africa



# The first Raman spectroscopic study of San rock art in the Ukhahlamba Drakensberg Park, South Africa

Linda C. Prinsloo,<sup>1\*</sup> Werner Barnard,<sup>2</sup> Ian Meiklejohn<sup>3</sup> and Kevin Hall<sup>3,4</sup>

<sup>1</sup> Department of Physics, University of Pretoria, Pretoria 0002, South Africa

<sup>2</sup> Department of Chemistry, University of Pretoria, Pretoria 0002, South Africa

<sup>3</sup> Department of Geography, Geoinformatics and Meteorology University of Pretoria, Pretoria 0002, South Africa

<sup>4</sup> Geography Department, University of Northern British Columbia, 3333 University Way, Prince George, BC., Canada, V2N 4Z9

Received 26 October 2007; Accepted 9 November 2007

San rock art sites are found throughout southern Africa; unfortunately this unique heritage is rapidly being lost through natural weathering processes, which have been the focus of various studies conducted in the Ukhahlamba Drakensberg Park since 1992. It has recently been shown that the ability of Raman spectroscopy to identify salts on rock faces on a micro, as well as nano scale, can make a contribution to these projects.

In order to test the feasibility of undertaking on-site analyses, a small rock fragment with red and white pigments still attached, which had weathered off the rock face, was analysed with Raman spectroscopy under laboratory conditions, using a Dilor XY Raman instrument and a DeltaNu Inspector Raman portable instrument. A small sample of black pigment (<1 mm<sup>2</sup>), collected from a badly deteriorated painting and a few relevant samples collected on site, were analysed as well. It was possible to identify most of the inorganic pigments and minerals detected with previous XRD and EDX measurements including whewellite and weddellite coatings, which could be a tool for carbon dating purposes. Two carotenoid pigments were detected for the first time in San rock art pigments. Animal fat was also observed for the first time on both red and white pigments, on the rock face adjacent to the paintings and in highest concentrations on the back of the rock fragment. The spectra quality makes successful on-site measurements a good prospect. Copyright © 2008 John Wiley & Sons, Ltd.

**KEYWORDS:** San rock art; weddellite; whewellite; haematite; red ochre; animal fat

## INTRODUCTION

San rock art sites are found throughout southern Africa; unfortunately this unique heritage is rapidly being lost through natural weathering processes as the paintings are mostly found in rocky shelters and underneath overhangs, which are exposed to the elements. This has led to various projects during which factors influencing natural weathering processes such as micro-climate, rock moisture and rock temperature have been studied.<sup>1–6</sup>

A knowledge of the chemical composition of the pigments and binders used by the San artists is essential for the interpretation of rock weathering studies. X-ray powder diffraction (XRD), energy-dispersive X-ray spectroscopy (EDX) and paper chromatography have previously been used to analyse these pigments.<sup>6–8</sup> The pigments and binders

mentioned in the literature were also tested in practical experiments for their mixing, colouring and weathering properties.<sup>9,10</sup> Although it is generally agreed that iron oxides were the pigments used to obtain the earth tones and carbon or manganese oxide the black colour, there is still much speculation about the nature of the white pigment, the type of binders used and paint application methods of the artists.

Raman spectroscopy has been used successfully to analyse pigments and substrata in pre-historic rock art and it has been shown that it could also be useful in the study of San rock art deterioration.<sup>11–17</sup> In this study we test the feasibility of undertaking on-site Raman measurements by first analysing a few samples under laboratory conditions.

## The Ukhahlamba Drakensberg Park (a UNESCO World Heritage site)

The Drakensberg (Dragon Mountains) is the highest part of a 1000-km long escarpment that forms the chief watershed of the southern African subcontinent and the border between South Africa and the mountain kingdom of Lesotho (see

\*Correspondence to: Linda C. Prinsloo, Department of Physics, University of Pretoria, Pretoria 0002, South Africa.  
E-mail: linda.prinsloo@up.ac.za



map in Fig. 1). The Zulu name Ukhahlamba (a barrier of spears) is descriptive of the formidable character of this mountain range, which has its highest elevation in the Giant's Castle area.<sup>18</sup> The approximately 30 000 painted images (between 100–4000 years old) in nearly 600 rock-shelters in the area is one of the primary reasons why the Ukhahlamba Drakensberg Park has qualified as a World Heritage Site.<sup>19</sup>

### San rock art

The origin and arrival of the nomadic San hunter-gatherers (also known as 'Bushman') in southern Africa is lost in the mist of time, but they were the only inhabitants of a large part of the interior of southern Africa for at least 8000 years and left behind a valuable heritage through their paintings and engravings. The animated figures depicted in San rock art participate in such activities as dancing, hunting, running and fighting – a first-hand record of the every day life of the hunters of the Stone Age (Fig. 2(a)). Further the verve, variety and engaging animation of the figures, with an overall impression of exuberant energy, are unique amongst prehistoric art. In the Drakensberg their artistry reached its pinnacle with delicate polychrome paintings, where every minute detail is painstakingly depicted.<sup>20,21</sup>

Findings based on 19th century ethnographical records and current research concerning the northern San still living in the Kalahari shows that a part of San art was associated with the trance experience of 'medicine men' or shamans, hence the trance dances and hallucinatory experiences of the shamans depicted in some of their paintings (Fig. 2(b)).<sup>20,21</sup>

In this Shamanistic interpretation not only the pictures, but also the rock face were important, the latter being perceived as a veil between the known and the mystical world. Painting, therefore became a ritual act and the paint was prepared under ceremonial circumstances. For instance, a woman had to heat *qhang qhang* (red ochre) at night during a full moon, then grind it to a fine powder and mix it with

fresh eland blood to make red pigments. In this way the painting itself had the power of the eland, a large antelope revered by the San as a key symbol of life and potency.<sup>20,21</sup>

### Samples

In this preliminary study the pigment colours most frequently used by the San, namely white, red and black were analysed under laboratory conditions. A small rock fragment (Fig. 3(a)), which had fortuitously weathered off the rock face (Barnes' shelter, Giants Castle), was used to analyse the red and white pigments. A minute piece of black pigment was collected (under licence) from a painting that has nearly disappeared from the rock face (Wilcox shelter, Giants Castle). A few control samples, such as red ochre, were also collected on site.

### EXPERIMENTAL

Raman spectra were recorded with a XY Raman spectrometer from Dilor (liquid nitrogen-cooled CCD), using the 514.5 nm (Coherent Innova 90 Ar<sup>+</sup> laser) and yellow 568 nm (Spectra-Physics Krypton Stabilite 2017 laser) lines as exciting radiation. In both cases the scattered light was collected through an Olympus confocal microscope with a long distance  $\times 50$  microscope objective. The laser power was kept below 10 mW at the sample to prevent sample degradation.

A hand-held DeltaNu Inspector Raman instrument (weight <3 kg), equipped with a 785 nm diode laser for excitation with a maximum output power of 120 mW, was used to record spectra of the same samples. The spectral resolution of the instrument is 8 cm<sup>-1</sup> and the spectral range 200–2000 cm<sup>-1</sup>.

A Bruker 113v Fourier transform infrared (FTIR) spectrometer was used to record mid-infrared transmission spectra of powdered samples (1 mg) pressed into KBr (100 mg) pellets. The resolution was 2 cm<sup>-1</sup> and 32 scans were signal-averaged in each interferogram.

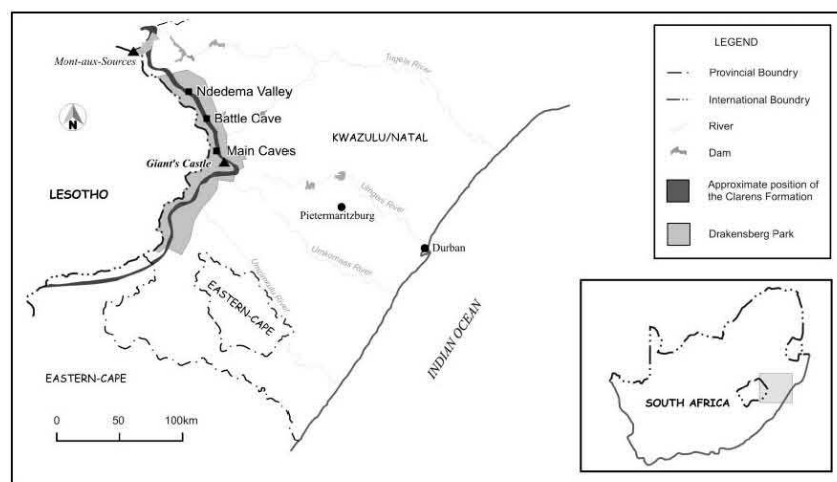
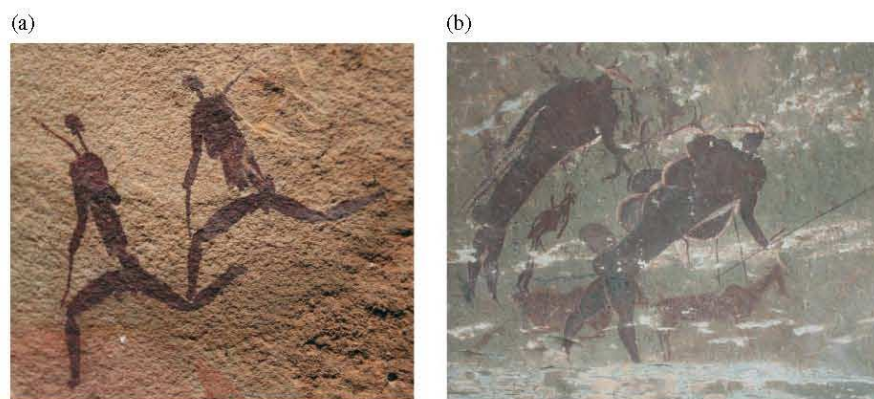
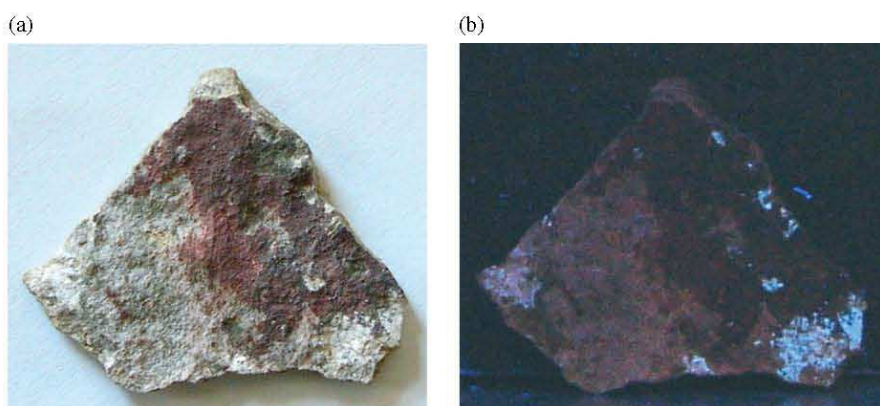


Figure 1. Map showing the Ukhahlamba Drakensberg Park in relation to the rest of South Africa.





**Figure 2.** San paintings: (a) two San hunters running; (b) two San shamans with eland heads and hooves (therianthropes: mythological part-man and part-beast figures) depicting the blending of man with the power of the eland. The bubbles around the one figure represent the experiences of shamans during trance dances when they feel the power exploding within them.



**Figure 3.** Photo of the shard with red and white pigment in (a) sunlight and (b) under 254 nm UV light.

X-ray diffraction data were collected using a PANalytical X'Pert Pro powder diffractometer with X'Celerator detector and variable divergence and receiving slits, with Fe filtered Co  $K_{\alpha}$ -radiation (35 kV 50 mA). Different phases were identified using X'Pert Highscore plus software. Quantification (Rietveld method) of the data was done by the Autoquan/BGMN software, (GE Inspection Technologies) employing the Fundamental Parameter Approach.

## RESULTS

### White pigment on shard

Fluorescence of the white pigment, as seen in the photo taken under 254 nm UV light (Fig. 3(b)), made Raman spectra difficult to obtain with the 514.5 nm laser line. Only by searching for a few specific spots without fluorescence, was it possible to record the well-known spectra of  $\alpha$ -quartz (126, 203 and 462  $\text{cm}^{-1}$ ) and two polymorphs of  $\text{TiO}_2$ , namely anatase (143 (vs), 395, 513 and 636  $\text{cm}^{-1}$ ) and rutile (230, 445 and 606  $\text{cm}^{-1}$ ).

### Red pigment on shard

Red particles in the pigment could be clearly distinguished from white and grey crystallites with the 50 $\times$  long distance objective of the Olympus microscope. Focusing on the grey and white crystallites, spectra of gypsum (strongest band 1007  $\text{cm}^{-1}$ ), as well as the anhydrous form anhydrite (1022  $\text{cm}^{-1}$ ),  $\alpha$ -quartz and the anatase phase of  $\text{TiO}_2$  were recorded.

The most prominent bands in almost all of the spectra recorded on the red particles of the pigment (Fig. 4) originate from calcium oxalate mono- (whewellite) or dihydrate (weddellite) or mixtures thereof. The two hydrates could easily be distinguished through the symmetric C=O stretch bands at 1462 and 1490  $\text{cm}^{-1}$  for whewellite (wh) and 1476  $\text{cm}^{-1}$  for weddellite (wd), as well as the C-C stretching vibration at 903 (wd) and 894  $\text{cm}^{-1}$  (wh). The well-defined lattice vibrations also clearly differentiate between the two hydrates as weddellite has two bands (164 and 196  $\text{cm}^{-1}$ ) and whewellite four bands (193, 203, 222 and 249  $\text{cm}^{-1}$ ) in this region.<sup>22</sup> The bands around 500 and 524  $\text{cm}^{-1}$  are due to Ca-O stretch vibrations, CaO ring deformation and O-C=O bending modes. Calcium oxalates are commonly found on



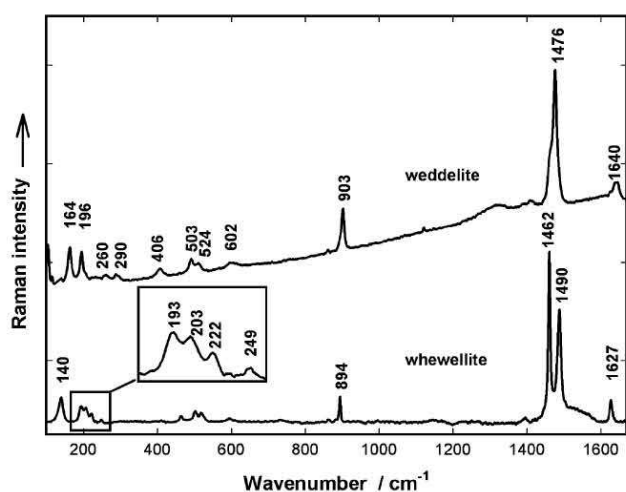


**Figure 4.** Examples of spectra recorded on the red pigment with the 514.5 nm laser line showing the hydrate phases of calcium oxalate.

calcite rock faces and has previously also been reported on sandstone.<sup>23,24</sup> In most of the spectra recorded on red parts of the sample, bands at 290, 406, 602 and  $\sim 1300$   $\text{cm}^{-1}$  are also present, which are characteristic of haematite. Although it could be expected that iron oxalates would form in the presence of oxalic acid, it was not detected.<sup>25</sup>

In Fig. 5 spectra recorded on the pigment are compared to spectra recorded for a red ochre found on the terrain and the ochre after it had been fired for 1 h at 650 °C (temperature of most wood-burning fires) in order to test the validity of the historical record of how the paint was produced ('San rock art'). The bands ascribed to haematite occur at the same positions in all the spectra and no shift is observed that can be attributed to heating or mixing of the pigment. The

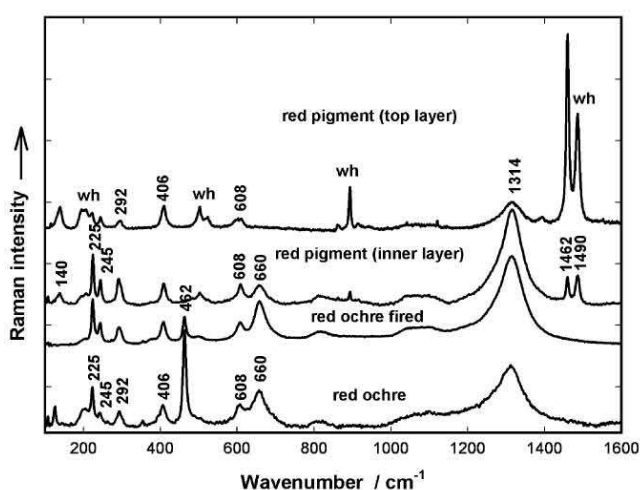


**Figure 5.** Spectra recorded on the red pigment on shard, red ochre and red ochre fired for 1 h at 650 °C. The spectrum of the top layer of pigment was obtained with a 514.5 nm laser line and the other spectra with a 568 nm laser line.

bandwidth of most of the peaks decreased with firing and six of the seven predicted Raman active first order modes of  $\alpha\text{-Fe}_2\text{O}_3$  (225, 245, 292, 409, 497 and 608  $\text{cm}^{-1}$ ),<sup>26</sup> as well as bands at 658 and 1314  $\text{cm}^{-1}$  are observed in all the spectra. In many papers the 658  $\text{cm}^{-1}$  band is assigned to magnetite, which normally occurs together with haematite in natural ochres and has its strongest band at this position. It has also been assigned to kaolinite in natural ochres.<sup>27</sup> In this case, however, the band still appears in the spectrum of the fired ochre (even stronger and narrower) where all the magnetite has been converted to haematite<sup>26</sup> and kaolinite has not been detected as seen from XRD analyses of the samples given in Table 1. In Refs 28–31 this band is assigned to an IR active mode which is symmetry forbidden in the Raman spectrum and its appearance in natural haematites ascribed to a lowering of symmetry in disordered structures. The two spectra recorded on the red paint differ first in the intensity of the bands originating from whewellite (1462 and 1490  $\text{cm}^{-1}$  most intense bands) relative to the intensity of the 406  $\text{cm}^{-1}$  band of haematite. As the spectrum with the weakest oxalate bands was recorded on a part of the paint where the outside layer has been scraped off, it appears that the oxalate was not part of the original pigment, but formed later over the paint layer. Second, the 1314  $\text{cm}^{-1}$  band in the spectrum recorded on the inside pigment layer is much stronger than in the spectrum recorded on the outermost layer. This probably is owing to a strong resonance enhancement of this band with 568 nm excitation, which have been observed for certain forms of haematite crystallites (platelets).<sup>30</sup>

Two types of spectra (Fig. 6) were recorded for the fired ochre on red crystallites (note that the spectra do not resemble the Raman spectra of any of the other compounds present in the ochre—Table 1). In one spectrum the intense bands are narrow and reminiscent of a highly crystalline material, while in the other most bands have broadened and shifted to

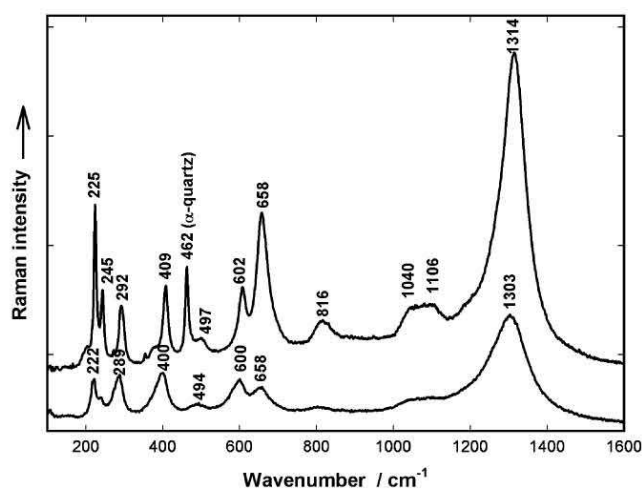


**Figure 6.** Comparison of two types of spectra recorded on the red particles of the ochre fired at 650 °C (both obtained with 568 nm excitation).

**Table 1.** XRD analysis of the red ochre and after firing at 650 °C (wt%)

	Red ochre rock	Red ochre fired
Calcite (CaCO <sub>3</sub> )	0.21	0.35
Haematite (Fe <sub>2</sub> O <sub>3</sub> )	0.84	1.28
Magnetite (Fe <sub>3</sub> O <sub>4</sub> )	0.68	0.06
Microcline, intermediate1 (KAlSi <sub>3</sub> O <sub>8</sub> )	2	2.65
Muscovite {KAl <sub>2</sub> (AlSi <sub>3</sub> O <sub>10</sub> )(OH) <sub>2</sub> }	12.43	8.11
Plagioclase (Na,Ca)(Al, Si) <sub>4</sub> O <sub>8</sub>	10.5	9.9
Quartz (SiO <sub>2</sub> )	73.35	77.64

lower wavenumbers. This could be due to differences in size, morphology or orientation of the pigment crystallites.<sup>29–31</sup> It has recently also been illustrated that doping with aluminium broadens and shifts most bands in the haematite Raman spectrum to lower wavenumbers, which might be another explanation for the existence of this second spectrum.<sup>32,33</sup> The origin of the band at 1314 cm<sup>-1</sup> has previously been attributed to a two magnon scattering process, but later work support a resonance-enhanced two-phonon process with the IR active band at 658 cm<sup>-1</sup> as fundamental.<sup>28,34</sup> Interestingly, although this band has shifted downwards to 1303 cm<sup>-1</sup>, the band at 658 cm<sup>-1</sup> is still in the same position. The rather broad bands at 816 and between 1040 and 1106 cm<sup>-1</sup> have previously also been noted in the spectra of a haematite single crystal and occur only in *xx* polarisation.<sup>29</sup>

Spectra similar to the second kind of haematite spectrum recorded on the fired sample were also obtained on the ochre and pigment on the shard (Fig. 7). A change in relative intensity and wavenumber to lower wavenumber

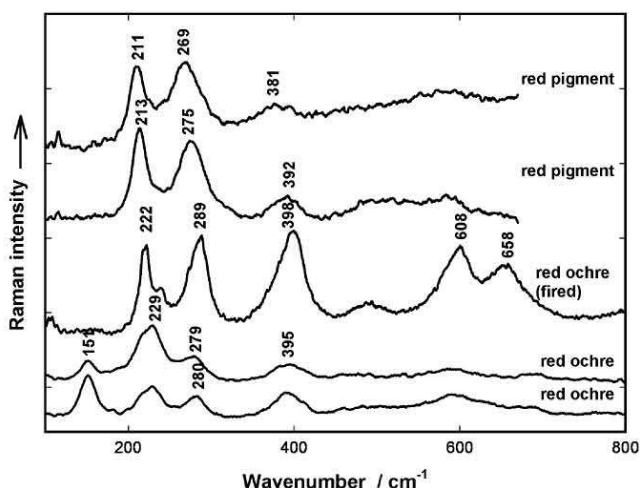


**Figure 7.** Comparison of the second kind of haematite spectrum as recorded on the red ochre, the ochre fired at 650 °C and on the pigment itself. All spectra recorded with 514.5 nm excitation, except for the spectrum of the fired sample, which was obtained with 568 nm excitation.

values is observed from the natural ochre to the pigment on the shard (the spectrum of the fired ochre was recorded with the 568 nm laser and therefore not directly comparable). It has been shown that the Raman spectrum of haematite is very dependent on particle size and morphology, production process, as well as the energy of the exciting radiation. In the formation process of clay many different processes can play a role to form heterogeneous mixtures and it is quite possible that more than one type of haematite may exist in a natural ochre sample.

### Back of shard

Gypsum was detected in most spectra recorded on the back of the shard and anhydrite in a few. Spectra of feldspar (252, 291, 330, 416, 480 and 508 cm<sup>-1</sup>),<sup>34</sup>  $\alpha$ -quartz, anatase and oxalates (wd and wh) were also recorded. It is suspected that sulphates, dissolved in surface water, accumulated at the back of the shard resulting in its detachment from the rock face.

### FTIR measurements of shard

The small size of the area analysed with Raman microscopy and the subjective choice of its location by the operator do not give a representative analysis of a sample and therefore transmission mid-infrared spectra were recorded for the samples. In Fig. 8 the spectra of the white pigment, red pigment, back side of the rock fragment and pristine Clarens formation sandstone are compared. The pigment samples were scraped off the top of the shard and therefore reflect the composition of the top layer. The strongest bands in spectra of both the red and white pigment, originate from whewellite (782, 1316 and 1624 cm<sup>-1</sup>),<sup>35</sup> but a band at 1655 cm<sup>-1</sup> (as yet unidentified) indicates that another organic phase is present in the white pigment. The spectrum recorded on the back of the shard has bands characteristic of  $\alpha$ -quartz (strongest peak  $\sim$ 1000 cm<sup>-1</sup> and characteristic doublet at 779 and 798 cm<sup>-1</sup>). All the other peaks are attributed to gypsum ( $\nu_3$  at 1150 cm<sup>-1</sup>,

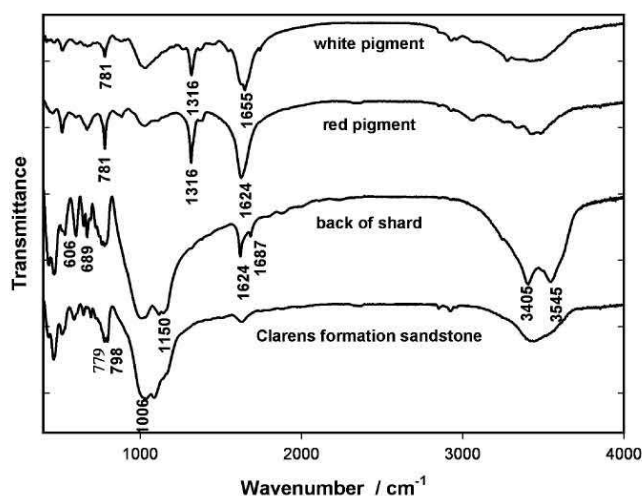


**Figure 8.** FTIR spectra recorded of white pigment, red pigment, back of the shard and Clarens formation sandstone.



$\nu_4$  at 606 and 689  $\text{cm}^{-1}$ , lattice water-stretching vibrations at 3405, 3545  $\text{cm}^{-1}$  and bending vibrations at 1624, 1687  $\text{cm}^{-1}$ ). Notice the absence of a peak at 1316  $\text{cm}^{-1}$  in the spectrum of pristine sandstone (only slightly visible in spectrum of the back of the shard), which indicates the absence of whewellite.

### Black pigment

The spectra presented in Fig. 9 were recorded on a very small sample of black pigment collected from a severely deteriorated painting and the two characteristic broad bands of amorphous carbon (1350 and 1600  $\text{cm}^{-1}$ ) can clearly be observed. In all the spectra, except one, whewellite and weddellite in varying concentrations were observed. It is notable that the peaks assigned to Fe–O vibrations in similar spectra recorded on the red pigment are absent. Calcite (1082  $\text{cm}^{-1}$ ), gypsum (1007  $\text{cm}^{-1}$ ) and anhydrite (1022  $\text{cm}^{-1}$ ) were also detected.

### Organic phases detected with 514.5 nm laser excitation

An organic phase was detected on the white pigment that can be attributed to a pigment of carotenoidal nature. In Fig. 10 the spectrum is compared to that of egg white, the yolk and a mixture. (Note that poultry eggs were used to record the spectra; the San would probably have used ostrich eggs). Egg white has been suggested as a binder for San rock art, but experimental studies have shown that egg white on its own has very poor binding properties. In contrast egg yolk is an excellent binder and has been used in the 'egg tempera' paintings of medieval frescoes.<sup>36</sup> The spectrum recorded on the red pigment closely resembles the spectrum of the egg yolk, with strongest bands due to lutein<sup>37</sup> (the carotenoid responsible for the yellow colour of the yolk) and could indicate that egg yolk (or a mixture) was used as a binder by the San artists. It is only circumstantial evidence though, as many other natural carotenoids have spectra similar to that of lutein

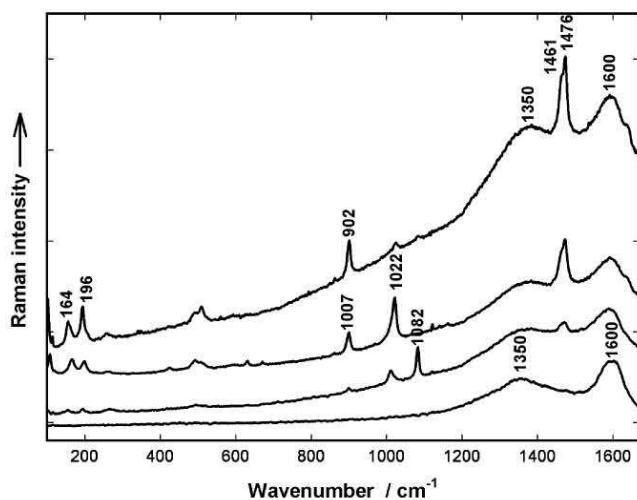


Figure 9. Various Raman spectra recorded on a small sample of black pigment.

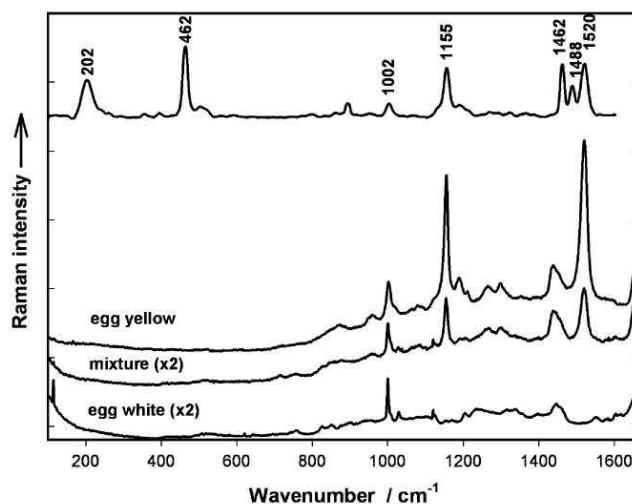


Figure 10. Organic phase detected in white pigment in comparison with spectra recorded from egg white, the yolk and a mixture.

and the presence of carotenoid pigments could also originate from lichens or other plant material. The other bands in the spectrum can be ascribed to whewellite and  $\alpha$ -quartz.

On the black pigment another compound of carotenoidal nature was observed with the two most intense bands at 1503 and 1148  $\text{cm}^{-1}$  assigned to the C=C and C–C stretching modes respectively (Fig. 11).<sup>39</sup> Also, many overtone and combination bands were observed at higher wavenumbers, which is characteristic of carotenoids due to the "carry over" of the resonance effect. The C=C stretching value of 1503  $\text{cm}^{-1}$  is significantly lower than that of many natural carotenoids that contain nine conjugated double bonds and compares well with the reported values of certain natural marine carotenoids that have unmethylated polyacetylenic backbones.<sup>40,41</sup> The C–C stretching vibration

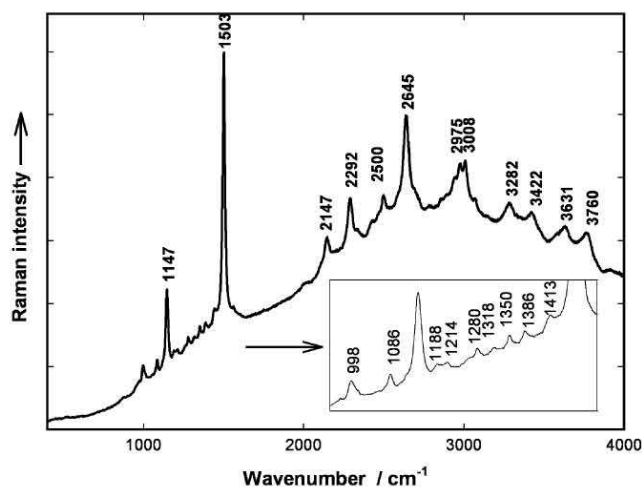


Figure 11. Resonance-enhanced spectrum of a carotenoid recorded with 514.5 nm laser line on the black pigment.

at  $1147\text{ cm}^{-1}$  is indicative of methyl substitution (average value of  $\sim 1155\text{ cm}^{-1}$  of other substituted carotenoids) rather than that of the unsubstituted carotenoids that have a value of  $\sim 1130\text{ cm}^{-1}$ .<sup>40</sup> It is therefore deduced that it is a methyl substituted carotenoid with a longer than normal conjugated backbone. The reported C–C and C=C stretching modes of two long chain carotenoids, decapreno- $\beta$ -carotene (at  $1504\text{ cm}^{-1}$  and  $1152\text{ cm}^{-1}$ ) and bacterioruberin (at  $1505\text{ cm}^{-1}$  and  $1152\text{ cm}^{-1}$ ) compare well with our data (Fig. 13).<sup>42,43</sup> The weaker bands reported for decapreno- $\beta$ -carotene at  $1002$  ( $\text{CH}_3$  deformation),  $1193$  ( $\text{CH}-\text{CH}$  deformation) and  $1283\text{ cm}^{-1}$  ( $\text{HC}=\text{CH}$  in-plane rocking) as well as the only other reported band for bacterioruberin at  $1000\text{ cm}^{-1}$  coincide with the corresponding bands in our spectrum. The C=C stretching band value is indicative of the effective conjugation length of polyacetylenic systems and applying the mathematical relationship reported in reference 39 to this carotenoid, predicts an effective conjugation length of approximately 12 conjugated double bonds. Decapreno- $\beta$ -carotene and bacterioruberin each have 13 formal conjugated double bonds in their polyacetylenic backbones and the lower value predicted is rationalised by the fact that the  $\text{CH}_3$  groups distort the backbone, lowering the effective conjugation length. Our carotenoid is probably not decapreno- $\beta$ -carotene, but rather similar in structure to bacterioruberin as it has been extensively reported to be produced in nature by many different halobacteria,<sup>43</sup> whereas the authors could to their knowledge find no reference to any natural occurrence of decapreno- $\beta$ -carotene. Supportive of this is the recent report that bacterioruberins have been detected on frescoe paintings.<sup>44</sup>

#### Results obtained with the portable instrument

On the red pigment, in agreement with the measurements with the XY instrument, bands originating from the two calcium oxalates were present in most spectra. The bands due to other inorganic phases (e.g. haematite) are very weak and not very useful.

Spectra recorded on the back of the shard (Fig. 12, bottom), had very strong bands clearly originating from an organic phase with the characteristic band of gypsum ( $1007\text{ cm}^{-1}$ ) also prominent. Animal fat has quite frequently been mentioned in the literature as a possible binder for San pigments and a spectrum of fat (beef) smeared on sandstone was also recorded (Fig. 12, middle). The five bands in the spectrum is very typical of a fat and can be assigned to a carbonyl stretch  $\nu(\text{C}=\text{O})$  at  $1738\text{ cm}^{-1}$ , a  $\nu(\text{C}=\text{C})$  stretch at  $1628\text{ cm}^{-1}$ , the  $\delta(\text{C}-\text{H})$  conformation vibration at  $1419\text{ cm}^{-1}$ , an in-phase methylene twisting deformation ( $1300\text{ cm}^{-1}$ ) and at  $1237\text{ cm}^{-1}$  the in-plane  $=\text{CH}$  deformation vibration.<sup>45</sup> The two spectra match perfectly (Fig. 12).

Animal fat was also detected on the red and white pigments, as well as on a rock fragment from the adjacent rockface. On the white pigment mixtures of anatase, whewellite as well as an unidentified organic phase (broad

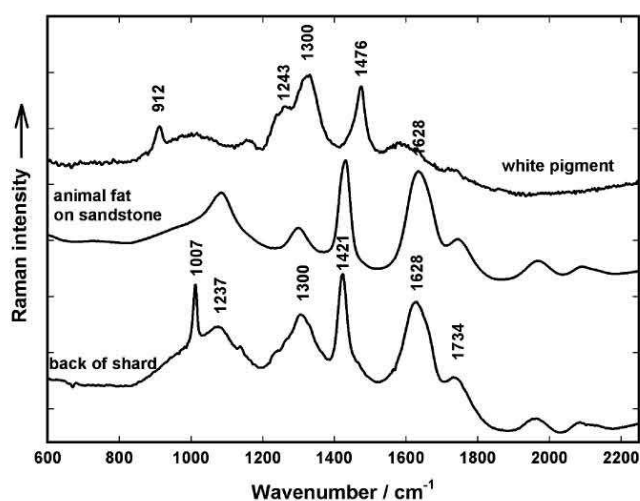


**Figure 12.** Spectra recorded on the back of the rock garment (bottom), animal fat on sandstone (middle) and the white pigment (top) with the  $785\text{ nm}$  laser line of the DeltaNu portable instrument.

bands  $\sim 1243$  and  $1300\text{ cm}^{-1}$ ), were also detected (Fig. 12, top). The black pigment sample was too small to record spectra on the portable instrument.

## DISCUSSION

The combination of the three laser lines and FTIR measurements gave complementary results, which are summarised in Table 2. It can be deduced that haematite (red ochre) was the pigment used for the red colour, carbon for the black and possibly a white clay or shale for the white colour. The white

**Table 2.** Summary of compounds detected on the various pigments and backside of rock fragment

Compound	Red pigment	White pigment	Backside	Black pigment
Carbon	*			***
Haematite	***			
Weddellite	***	***		***
Whewellite	***	***	*	***
Gypsum	**	*	***	*
Anhydrite	*		*	
Feldspar	*		**	
$\alpha$ -quartz	**	**	**	**
Calcite	*	*	*	**
Rutile		*		
Anatase	*	**	*	*
Animal fat	*	**	***	not recorded

\*\*\* Present in most spectra recorded.

\*\* in some spectra.

\* in one spectrum.





pigment contains a still unknown organic phase, which is fluorescent.

Weddellite and whewellite were detected everywhere on the shard, but in highest concentrations on the pigments. The much lower intensity of bands originating from the oxalates in spectra recorded on the red pigment, where the top layer has been scraped off, suggests that it was not part of the original pigment. The detection of oxalates on the pigments may open a window to date the paintings more accurately, especially if the pigment is encapsulated between two oxalate layers as found for pigments in Spain and Texas, which protect the paint, prevent weathering and have been used for AMS  $^{14}\text{C}$  dating of Post-Paleolithic rock art.<sup>23,24</sup> The origin of the oxalic acid necessary to form the oxalates has been ascribed to previous colonisation of the rock face by lichens, but it has been shown that the presence of rock hyraces in shelters may also be a source of oxalic acid.<sup>17</sup> Furthermore, it is suspected that San artists used plant sap as binder and as many plants have oxalic acid as a constituent of the sap it may have been introduced into the paint in this way as suggested in Ref. 5.

The ability to detect very low concentrations of carotenoid pigments with the green laser line due to the resonance effect is very useful. A careful study of the microenvironment of a painting would be necessary to determine if the presence of the carotenoids is due to deliberate addition by the artists or the previous/later presence of lichens, fungi or algae on the rock face.

Many authors have speculated that San artists used animal fat as binder and it is still used for the preparation of cosmetic and ritual body paint in San communities in the Kalahari.<sup>10</sup> Practical experiments have also shown that ochre mixed with animal fat has good weathering properties, but it is very difficult to draw the delicate lines that San rock art is famous for with such a mixture.<sup>9,10</sup> The concentration of fat on the back of the rock fragment, suggests that the surface of the rock face was first prepared for painting by covering it with fat (probably hot), which would penetrate into the sandstone and prevent the paint from soaking into it. It can however not be overlooked that the fatty layer might have another origin. Humans (other than the San) have for long periods of time occupied shelters like Barnes' shelter, where the shards were collected. (The first game ranger of the Giant's Castle Nature Reserve, Mr Barnes used the shelter as his head quarters). The fatty layer might therefore originate from cooking activities in the shelter. Rock hyraces have also inhabited the shelters and as they produce volatile short-chain fatty acids as part of their metabolic products they could also have contributed to an organic coating on the rock face.<sup>17</sup>

Unfortunately the fatty layer would also hinder the natural flow of groundwater through the sandstone and bring about an accumulation of soluble salts, such as sulphates behind the fatty layer (Fig. 10 supports this), which would

cause the layer with the applied pigment to detach from the rock face with time.

Attempts to verify the account of how the paint was produced (firing and mixing with eland blood) has so far been unsuccessful. An in-depth study of the temperature behaviour of the natural ochres found on the terrain might provide an answer to the question if the ochres were fired before mixing the paints.

## CONCLUSION

The weathering of the rock faces depicting San rock art is a complex mechanism encompassing interdependent mechanical, geological, chemical, physical and biological processes. We have shown that Raman spectroscopy could play a very useful role in unravelling the key factors that contribute to this process. As each individual rock art site has a unique microclimate, which influences the stability of the paints, an on-site study of each site will be necessary to make an input in the decision-making process for its preservation. In the same way the interpretation of the data collected on rock paintings has to be done in relation to the micro-environment of each painting, as well as the historical record of the site. The discovery of animal fat on the rock fragment collected from Barnes' shelter is exciting, but the exact origin of the fat has to be verified by similar experiments at other sites.

## Acknowledgements

The authors wish to thank Heritage KwaZulu-Natal (permits 04/26 and 04/27) for permission to collect samples, Sabine MC Verryn (XRF and XRD Laboratory, University of Pretoria) for taking the XRD measurements and Stéphane Hoerlé (Rock Art Research Centre, University of the Witwatersrand) for his comments on the manuscript.

## REFERENCES

1. Meiklejohn I. S. *Afr. Geogr. J.* 1997; **79**: 199, Special issue.
2. Hoerlé S, Salomon A. S. *Afr. J. Sci.* 2004; **100**: 340.
3. Hoerlé S. S. *Afr. J. Geol.* 2005; **108**: 297.
4. Hoerlé S. *Earth Surf. Processes Land.* 2006; **31**: 383.
5. Hall K, Meiklejohn I, Arocena JM. *Geomorph.* 2007; **91**: 132.
6. Arocena JM, Hall K, Meiklejohn I. *J. Geoarchaeol.* in press.
7. van Rijssen WJ. *S. Afr. Archaeol. Bull.* 1990; **45**: 58.
8. Denninger E. S. *Afr. J. Sci. Spec. Publ.* 1971; **2**: 80.
9. Johnson T. S. *Afr. Archaeol. Bull.* 1957; **12**: 98.
10. Rudner I. S. *Afr. Archaeol. Soc. Goodwin Ser.* 1983; **4**: 14.
11. Zoppi A, Signorini GF, Lucarelli F, Bachechi L. *J. Cult. Herit.* 2002; **3**: 299.
12. Smith DC, Bouchard M, Lorblanchet M. *J. Raman Spectrosc.* 1999; **30**: 347.
13. Edwards HGM, Drummond L, Russ J. *Spectrochim. Acta, Part A* 1998; **54**: 1849.
14. Edwards HGM, Drummond L, Russ J. *J. Raman Spectrosc.* 1999; **30**: 421.
15. Hernanz A, Mas M, Gavilán B, Hernández B. *J. Raman Spectrosc.* 2006; **37**: 492.
16. Ospitali F, Smith DC, Lorblanchet M. *J. Raman Spectrosc.* 2006; **37**: 1063.



17. Prinsloo LC. *J. Raman Spectrosc.* 2007; **66**: 1123.
18. Liebenberg DP. *The Drakensberg of Natal*. Cape & Transvaal Printers Ltd: Cape Town, 1972.
19. Mazel AD, Watchman AL. *Antiquity* 1997; **71**(272): 445.
20. Lewis-Williams JD. *Afr. Arts* 1985; **18**(3): 54.
21. Lewis-Williams JD, Dowson TA. *S. Afr. Archaeol. Bull.* 1990; **45**: 16.
22. Frost RL, Weier ML. *J. Raman Spectrosc.* 2003; **34**: 775.
23. Russ J, Kaluarachchi WD, Drummond L, Edwards HGM. *Stud. Conserv.* 1999; **44**: 91.
24. Hernanz A, Gavira-Vallejo JM, Ruiz-López JF. *J. Optoelectron. Adv. Mater.* 2007; **9**: 512.
25. Edwards HGM, Russell NC. *J. Mol. Struct.* 1998; **443**: 223.
26. De Faria DLA, Silva SV, de Oliviera MT. *J. Raman Spectrosc.* 1997; **28**: 873.
27. Bikiaris D, Danilia Sister, Sotiropoulou S, Katsimbiri O, Pavlidou E, Moutsatsou AP, Chryssoulakis Y. *Spectrochim. Acta, Part A* 1999; **56**: 3.
28. McCarty KF. *Solid State Commun.* 1988; **68**: 799.
29. Bersani D, Lottici PP, Montenero A. *J. Raman Spectrosc.* 1999; **30**: 355.
30. Wang J, White WB, Adair JH. *J. Am. Ceram. Soc.* 2005; **88**(12): 3449.
31. Chernyshova IV, Hochella MF Jr, Madden AS. *Phys. Chem. Chem. Phys.* 2007; **9**: 1736.
32. Zoppi A, Lofrumento C, Castellucci EM, Sciau Ph. *J. Raman Spectrosc.* 2008; **39**: 40.
33. Froment F, Tournié A, Colomban Ph. *J. Raman Spectrosc.* in press.
34. Gillet P. *Applications of Vibrational Spectroscopy to Geology in Handbook of Vibrational Spectroscopy* (eds). Chalmers EM, Griffiths PR, John Wiley & Sons Ltd: London 2002; 3169–3191.
35. Petrov I, Šoptrajanov B. *Spectrochim. Acta* 1975; **31A**: 309.
36. Lepot L, Denoël S, Gilbert B. *J. Raman Spectrosc.* 2006; **37**: 1098.
37. Hoskins LC. *Spectrochim. Acta* 1986; **42A**(2/3): 169.
38. Barnard W, de Waal D. *J. Raman Spectrosc.* 2006; **37**: 342.
39. Saito S, Tasumi M. *J. Raman Spectr.* 1983; **14**: 310.
40. Barnard W, de Waal D. *J. Raman Spectr.* 2006; **37**: 342.
41. Karampelas S, Fritch E, Mevellec J-Y, Gauthier J-P, Sklavounos S, Soldatos T. *J. Raman Spectr.* 2007; **38**: 217.
42. Veronelli M, Zerbi G, Stradi R. *J. Raman Spectr.* 1995; **26**: 683.
43. Marshall CP, Leuko S, Coyle CM, Walter MR, Burns BP, Neilan BA. *Astrobiology* 2007; **7**: 631.
44. Imperi F, Caneva G, Cancellieri L, Ricci MA, Sodo A, Visca P. *Environ. Microbiol.* 2007; **9**: 2894.
45. Vandenaabee P, Wehling B, Moens L, Egwards H, De Reu M, Van Hooydonk G. *Anal. Chim. Acta* 2000; **407**: 261.